

# GENETIC AND BIOCHEMICAL CHARACTERIZATION OF $\lambda$ SPANIN

An Undergraduate Research Scholars Thesis

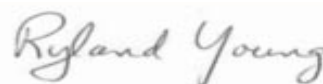
by

ANEESHA KULKARNI

Submitted to Honors and Undergraduate Research  
Texas A&M University  
in partial fulfillment of the requirements for the designation as an

UNDERGRADUATE RESEARCH SCHOLAR

Approved by  
Research Advisor:



Dr. Ryland Young

May 2014

Major: Genetics  
Computer Engineering

# TABLE OF CONTENTS

	Page
ABSTRACT.....	1
ACKNOWLEDGEMENTS .....	2
NOMENCLATURE .....	3
CHAPTER	
I INTRODUCTION .....	4
II MATERIALS AND METHODS.....	8
Strains and growth conditions.....	8
Screening for non-functional spanin mutants .....	8
DNA transformation and site directed DNA mutagenesis.....	8
SDS-PAGE and Western Blotting .....	9
Phage titer, phage plating, phage isolation and phage lysogenization.....	10
III RESULTS .....	12
Separation of <i>Rz</i> and <i>RzI</i> in the $\lambda$ chromosome .....	12
Isolation of <i>Rz</i> and <i>RzI</i> mutants.....	13
Genetic characterization of the Spanin mutants.....	15
Biochemical characterization of the Spanin mutants.....	15
Mutants of <i>Rz</i> and <i>RzI</i> form a complex .....	16
IV DISCUSSION .....	18
REFERENCES .....	22
APPENDIX.....	24

## ABSTRACT

Genetic and biochemical characterization of  $\lambda$  spanin. (May 2014)

Aneesha Kulkarni  
Department of Biochemistry and Biophysics  
Texas A&M University

Research Advisor: Dr. Ryland Young  
Department of Biochemistry and Biophysics

The  $\lambda$  lysis genes *Rz* and *RzI* play an important role at the final step of bacterial cell lysis. *Rz* encodes an integral inner membrane protein and *RzI* encodes an outer membrane lipoprotein. These two proteins form a complex that spans the periplasm and thus the term spanins. Previous studies had made it clear that both of these proteins are required for the outer membrane disruption, however its mode of action is still unclear. On the other hand, due to its unusual genetic architecture where *RzI* allele is entirely embedded within *Rz* allele at +1 reading frame, thorough genetic analysis was intractable. Here we report our approach of separating these two complementary genes in the lambda lysis cassette. In parallel, a collection of both *Rz* and *RzI* mutants were isolated in order to better understand their role in lysis. The isolated mutants were tested for their expression *in-vivo*. Our attempt to further characterize their biochemical role is still in progress. Similarly, isolating the intergenic or intragenic suppressor of the mutants under study is also in progress.

## **ACKNOWLEDGEMENTS**

I would like to thank my advisor Dr. Ryland Young for giving me the opportunity to work on this project. I would also like to thank my mentor Manoj Rajaure for his guidance and input throughout this project.

## NOMENCLATURE

IM	Inner membrane
OM	Outer Membrane
OD	Optical Density
LB	Luria-Bertani
PVDF	Polyvinylidene Difluoride
BME	$\beta$ -mercaptoethanol

# CHAPTER I

## INTRODUCTION

The  $\lambda$  lysis cassette consists of a cluster of four genes namely *S*, *R*, *Rz* and *RzI* in order (Fig.1). All four genes are essential for phage lysis. The *S* and *R* genes code for the  $\lambda$  holin and endolysin, respectively. When accumulated to a critical concentration over time, the holins create large non-specific holes in the inner membrane (IM). This initializes the phage lysis process by allowing the endolysin, a transglycosylase, to escape the cytoplasm. The escape of endolysin into the periplasm results in the degradation of its substrate, the peptidoglycan. The distal genes, *Rz* and *RzI* have a unique genetic architecture in that they share the same DNA but exist in separate reading frames. This unusual pair of *Rz* and *RzI* genes code for an integral inner membrane protein called the i-spanin and an outer membrane lipoprotein called the o-spanin, respectively. Both i-spanin and o-spanin are required for the disruption of the outer membrane completing the final step in phage lysis (Berry et al., 2012) (Figure 2). However, the mechanistic role of neither *Rz* nor *RzI* in the disruption of outer membrane is yet understood. The complexity of its genetic architecture, as *RzI* is completely embedded within *Rz* at +1 register, has limited our ability for the genetic analysis of  $\lambda$  spanins.

The *Rz* gene encodes an integral inner membrane protein (i-spanin) and is 153 amino acids long. This protein extends into the periplasm while being tethered to the inner membrane by a transmembrane domain (Figure 1) at its N-terminus. Its periplasmic domain consists of two predicted  $\alpha$ -helical structures based on secondary structure analysis of the protein. These  $\alpha$ -helical regions are predicted to have a strong tendency to form a coiled-coil structures. The *Rz* protein also forms covalently linked homodimers *in vivo*, utilizing the two cysteine residues at

positions 99 and 152, a process catalyzed by the host Dsb system. (Berry et al., 2013). However, the purpose of these intermolecular linkages in the functioning of the spanin is still unclear.

The *RzI* gene is first translated into a 60 amino acid long pro-lipoprotein. After the cleavage of its 20-residue long signal sequence at the N-terminus, the cysteine at position 20 is modified. Modification of this N-terminus cysteine residue with three lipid groups is followed by the localization of this protein in the outer membrane by the Lol-system of the host (Kedzierska et al., 1996). The mature form of Rz1 is a 40 amino acid long poly-proline rich peptide (Fig. 1), which is attached to the outer membrane. There is no predicted secondary structure for Rz1 mainly due to the 25% proline residue content in the mature protein. Similar to Rz, Rz1 also exists as a covalently linked homodimer. The cysteine at position 29 is involved in the formation of the intermolecular disulfide bond between the Rz1 monomers. While it is not required that all three disulfide bonds be present for efficient functioning of the spanin, at least one of the covalent disulfide bonds (either in Rz<sub>152</sub> or in Rz<sub>129</sub>) must be present in order for the spanin to be functional (Berry et al., 2013).

The interaction between Rz and Rz1 based on various lines of genetic, physiological and molecular evidence suggested that the Rz and Rz1 complex spans the periplasm connecting the inner membrane with the outer membrane (Berry et al., 2008; Zhang and Young, 1999). Recent biochemical and biophysical studies have shown that mixing of the soluble periplasmic domains of the Rz and Rz1 proteins (sRz and sRz1 respectively) results in the formation of rod-shaped sRz-sRz1 complexes, which have the length matching the width of the *E.coli* periplasm (Berry et al., 2010).

*Rz* and *RzI* equivalents are found in almost all dsDNA bacteriophages infecting Gram-negative bacteria (Summer et al., 2007) . The genetic architecture of these spanin equivalents is not limited to the embedded type as in the case of  $\lambda$ . Recent bioinformatic analyses provide evidence of functional spanins that are overlapped (as in phage P2) as well as those that are separated (as in phage T4). In phages where *Rz/RzI* equivalents were not found, single genes encoding proteins (termed u-spanins or unimolecular spanins) with the same functionality as the *Rz* and *RzI* proteins were identified as in the case of the T1 phage gene *gpII*. The existence of such spanin analogues in nature supports the importance of the spanin in lysis by disrupting the OM. However, the mechanism for the disruption of the OM by spanin is unclear. The current model for the disruption of the OM is by causing the fusion between IM and OM after the degradation of the peptidoglycan (Berry et al., 2013). This implies that there are multiple steps involved in the pathway of spanin function that are yet to be determined.

The genetic and biochemical evidence suggest that the interaction between *Rz* and *RzI* is necessary for the spanin function; however the exact constituent residues for this interaction have not yet been determined. In addition the other unknown intermediate states of spanin function are not known either. This study uses a genetic approach to isolate various mutants that could block any steps involved in the spanin function. This is coupled with the biochemical characterization of isolated non-functional *Rz* and *RzI* mutants to better understand the defects. In parallel, in this study, the embedded  $\lambda$  *RzRzI* genes are replaced with synthetic *RzRzI* alleles that are now separate and no longer identical at the DNA sequence level. Unlike in embedded genes, this allows us to introduce a single mutation either in *Rz* or *RzI* of  $\lambda$  chromosome without affecting



the other gene. The objective of this separation of *Rz* and *RzI* gene was to isolate suppressors of the characterized mutants.

## **CHAPTER II**

### **MATERIALS AND METHODS**

#### **Strains and growth conditions**

The strains and their relevant genotypes used in this study are listed in the Table 1. Bacterial cultures were grown in standard Luria-Bertani broth (LB) media with addition of MgSO<sub>4</sub> (5mM), ampicillin (100 µg ml<sup>-1</sup>) and kanamycin (40 µg ml<sup>-1</sup>) final when applicable. The cultures were grown under standard laboratory condition with vigorous shaking at 250 rpm. Growth of the bacterial culture was monitored by recording absorbance at 550nm (A<sub>550</sub>) as a function of time. Overnight cultures were diluted 300 fold in 25 ml of LB and grown at 30°C in 250 ml growth flasks until the growth reached the exponential phase of OD ~0.25. At this point the cultures were shifted to a 42°C water-bath for thermal induction for 15 minutes followed by continuous growth at 37°C.

#### **Screening of non-functional spanin mutants**

The mutant library of spanins generated by error-prone PCR method was screened for loss of spanin function. Briefly, the sub-cloned spanin mutant library was transformed into a λ lysogen having a defective spanin allele. The transformants that were unable to complement for the defective spanin in the λ prophage were enriched to isolate the plasmid. Isolation of the plasmid was done using the QIAprep Spin Miniprep Kit by the standard mini-prep technique described by the manufacturer (Qiagen, Chatsworth, CA). The plasmid was sent for sequencing to Eton BioScience Inc. (San Diego, CA) in order to identify the location of the mutation.

### **DNA transformation, DNA manipulation and site directed DNA mutagenesis.**

The DNA transformation procedures were performed as described previously (Smith et al., 1998). In short, plasmid DNA of approximately 60ng was mixed with the thawed competent cells and incubated in ice for 30 minutes. This was followed by heat shock at 42°C for 42 seconds followed by incubation in ice for another 2-3 minutes. After incubation, 1 ml of standard LB media was added to the mixture and incubated at 37°C for 1 hour. Following this, the culture was plated on LB plates with appropriate antibiotics for selection and placed in 37°C or 30°C overnight depending on whether or not the host carried a temperature sensitive repressor allele.

Primers, listed in Table 2, for site directed mutagenesis were designed using the synthetic spanin allele created previously as a template. The primers were designed such that there were 10-11 bases flanking each side of the desired mutation, the GC content of the primer was greater than 40% and the melting temperature was less than 70°C. The primers were obtained from Integrated DNA Technologies (Coralville, IA) and were used for site-directed mutagenesis using a QuikChange Site-Directed Mutagenesis Kit as described by the manufacturer (Agilent Technologies Inc., La Jolla, CA).

### **SDS-PAGE and Western Blotting**

SDS-PAGE and Western blotting were both performed as detailed previously (Bernhardt et al., 2002; Schagger and von Jagow, 1987). Briefly, 50 min post thermal induction of the lysogens, the protein was precipitated by adding 1ml aliquot of the culture to concentrated trichloroacetic acid (TCA) to a final concentration of 10% (v/v) over ice. The mixture was then centrifuged for 5 minutes and washed twice with acetone. The protein pellets were then left to air-dry overnight and resuspended in non-reducing 1X SDS-PAGE buffer (50 mM Tris-HCl, 2% SDS, 5%

glycerol, pH 6.8). The resuspension volume was normalized to 10µl per 0.1OD unit of culture taken when the culture aliquot was added to TCA. The protein samples were then loaded and resolved on a 16% polyacrylamide SDS-Tricine gel. The proteins obtained were transferred to a polyvinylidene difluoride (PVDF) membrane. This membrane was then placed in a 4% milk buffer (blocking solution) overnight. The proteins were then probed with a primary antibody against Rz and Rz1 separately at a dilution of 1:1000 and placed on a shaker at room temperature for 1 hour after which the membrane was washed using appropriate buffers. The secondary antibody, goat-anti-rabbit IgG conjugated to horseradish peroxidase was used at 1:5000 dilutions and added to the membrane. Treatment with secondary antibody for an hour was followed by washing with appropriate buffers prior to the development of the blot using SuperSignal West Femto Maximum Sensitivity Substrate kit (Thermo Scientific, Rockford, IL). The proteins were then visualized for chemiluminescence using the Bio-Rad XR Gel Doc System (Hercules, CA).

### **Phage titer, phage plating, phage isolation, and phage lysogenization**

The phage titer was roughly estimated using a spot titer method. The overnight culture of host strain MC4100 grown in TBM was brought to 5mM MgSO<sub>4</sub> final concentration. The culture (100uL) was then mixed with H-top TB agar and briefly vortexed and plated on a warm TB agar plate and left to solidify. Serially diluted phage lysate (up to 10<sup>9</sup> fold) in a λ dilution buffer was then spotted (5 µl spots) on this plate and incubated overnight at 37°C. The phage titer was then calculated based on the dilution factor that gives the least number of individual isolated plaques.

$$\text{Titer} = (\text{number of plaques}) \times 200 \times (\text{dilution fold}) \text{ pfu/ml.}$$

Phage plating was done by infecting 100µl of the host, MDS-12 (grown overnight), with an appropriate phage dilution and incubated at room temperature for 30 minutes. Following incubation, the mixture was then mixed with H-top TB agar and plated on warm TB plates and then incubated overnight at 37°C. The plaques obtained from this step were then picked based on experimental needs i.e. small plaques in the case of mutant isolation and large wild-type plaques in the case of suppressor isolation (Figure 5).

For phage lysogenization, 100uL of the overnight host culture of MDS-12 was infected with a phage dilution to an MOI of 0.1 and incubated at room temperature for 30 minutes. Standard LB media (1 ml) was then added to the mixture and incubated in 30°C for an hour. Following incubation, the cells were harvested by centrifugation of the mixture and then resuspended in a small volume (~100 µL) of residual LB from the supernatant. The entire harvested culture was then plated on LB plates with appropriate antibiotics to select for lysogens and incubated overnight at 30°C.

## CHAPTER III

### RESULTS

#### Separation of *Rz* and *RzI* in the $\lambda$ chromosome

Due to the complications associated with the embedded architecture of the *Rz/RzI*, the *spanin* genes had to be separated in order to be able to study the effects of mutations in *Rz* and *RzI* separately. Hence a plasmid containing the lysis cassette with separated *Rz/RzI* genes was created. This plasmid was later used for recombination purposes to swap with the parental  $\lambda$  lysis cassette. The available pR' plasmid cloned with synthetic alleles of *Rz* and *RzI* in tandem was used as a template to amplify the synthetic *Rz-RzI* fragment. Primers were designed such that they were homologous in frame to the chromosomal upstream sequence of  $\lambda$  *Rz* and downstream sequence of  $\lambda$  *RzI* respectively. The PCR product using these primers was used as a mega-primer to amplify the plasmid pNZ20SRR*RzRzI* that consists of entire  $\lambda$  lysis cassette with embedded *RzRzI* and the deletion substitution of *bor* gene with Kan resistance marker. The new construct of pAK1 was constructed using PCR with a megaprimer (Barik, 2002) (Fig 3a). The pAK1 plasmid now harbors the synthetic *Rz* and *RzI* alleles that are now separated. The newly constructed pAK1 plasmid was used to transform a  $\lambda$  lysogen containing the parental  $\lambda$  prophage. The resulting transformants were selected for kanamycin resistance as the pAK1 plasmid carried the kanamycin resistance marker in the *bor* gene. The transformants were later induced for phage production and the lysate was used to re-lysogenize a prophage free MDS-12 host. The kanamycin resistant lysogen would have resulted from the phage infection that originated from the recombination between the plasmid and the phage chromosome in the earlier step (Fig.3b). In order to isolate the  $\lambda$  recombinant with separate *Rz/RzI* genes, a phage lysate was prepared by inducing the lysogenized host to undergo lysis. The pickate that was isolated after plating the

lysate (using a suitable dilution) was used as a template to verify the separation of *Rz* and *RzI* by PCR Figure 3.c. The larger band size corresponds to the separated spanin allele size. Hence the *Rz* and *RzI* alleles are now separated and no longer share the same DNA as before.

Our next objective was to introduce mutations in either *Rz* or *RzI* allele of the synthetic plasmid using the previously mentioned DNA manipulation techniques. As of now, we have been able to create 7  $\lambda$  phages altogether with a mutation in either *Rz* or *RzI* (Table 2). We observed the plaque sizes of the mutant spanin alleles and those of the wild-type (separated or embedded) and noted a marked difference in sizes as the former resulted in punctiform plaques while the latter formed larger plaques under the same conditions (Figure 4).

After engineering the mutants, we aimed to isolate the suppressors of either mutant, which results in the formation of large plaques. Our method of isolating suppressors by increasing selective pressure, using a higher concentration of  $\text{MgSO}_4$  to stabilize the OM, has so far resulted in the generation of true revertants only. The other approach of irradiating the mutant phage lysate in bulk with UV light has not resulted in the generation of suppressors either.

### **Isolation of *Rz* and *RzI* mutants**

Using the method of error-prone PCR (Cirino et al., 2003), two separate mutant pools for *Rz* and *RzI* were created. Isolation of mutants from either pool was necessary to study the role of individual mutations that have any effect on spanin-mediated lysis. In order to isolate the *Rz* mutants, the pool was first transformed into a  $\lambda$  lysogen containing the *Rz<sub>am</sub>* mutation. Any missense mutation from the pool that affects the functioning of *Rz* would result in a defect in

lysis, else it would complement for the *Rz<sub>am</sub>* of the lysogen for lysis. The cells that fail to lyse would remain in the pool in their fragile spherical form and can be harvested by slow centrifugation. The plasmids isolated from harvested cells would enrich the *Rz* mutant pool. The same approach was applied to enrich for *RzI* mutant where a  $\lambda$  lysogen containing *RzI<sub>am</sub>* was used instead to select for mutants. After the enrichment process, each mutant pool was transformed into XL1-Blue competent cell to isolate individual plasmids from the pool and later sequenced to identify the position of the mutation in either the *Rz* or *RzI* allele.

From the 300 screened mutants of *Rz* and 200 for *RzI*, we were able to isolate 16 *Rz* mutants and 10 *RzI* mutants, each with a single missense change (Table 3). Our objective was to mutagenize *Rz* and *RzI* to the saturation level in order to account for every possible missense change that would result in a defect in function. The saturation level can be estimated by the coverage of any given gene for all possible nonsense mutations that require a single nucleotide change, assuming that all nonsense mutants will be null alleles. In the case of *Rz*, out of the possible 45 such sites of nonsense mutations, the maximum number of mutants identified was 17 giving a saturation level of 37.78% (Figure 6, upper panel). For *RzI*, out of the possible 17 sites, only 6 mutants were identified giving a saturation level of 35.29% (Figure 6, lower panel). An attempt to identify more nonsense mutations and subsequently increase the saturation level resulted in a repetition of the previously identified missense mutants or nonsense mutants.

The isolated mutants were further tested to confirm their non-functionality by performing a complementation assay. All the mutants failed to cause lysis except the *Rz* mutants R83H and



K96I, which showed wild-type behavior (Table 3). The representative growth curves for characterized mutants of *Rz* and *RzI* are shown in Figure 5.

### **Genetic Characterization of the Spanin mutants**

The non-functional mutants isolated previously were further tested to check for dominance against the wild-type parental lysis cassette. If the mutation was able to affect the existing wild-type spanin present in the lysogen, then we would expect the cultures to exhibit a lysis defect and hence the mutation would be termed a dominant negative; otherwise, the allele would be judged to be recessive. Each mutant of *Rz* or *RzI* allele cloned in pRE plasmid was transformed into a  $\lambda$  lysogen (with the parental lysis cassette) using DNA transformation procedures. The transformants were tested by thermally inducing the  $\lambda$  prophage and subsequently inducing the expression of the mutant *Rz* or *RzI* proteins from the transformed plasmid. All the test inductions failed to block lysis in the presence of a mutant copy of either *Rz* or *RzI* (Table 3, a & b), suggesting that all the isolated mutant alleles of *Rz* and *RzI* were phenotypically recessive.

### **Biochemical Characterization of the Spanin mutants**

The genetic analysis of each isolated mutant failed to cause lysis except R83H and K96I. These two mutants were first isolated in the mutant pool, which after separation from the pool tested to be functional as wild type. The remaining mutants that were tested negative in terms of function also turned out to be recessive. Therefore, it was important to provide the biochemical evidence for the expression of mutant proteins *in-vivo*. The TCA precipitates of each *Rz* or *RzI* mutant expression was compared with the wild type expression level by running a SDS-PAGE gel under non-reducing condition followed by western blotting that was probed against *Rz* or *RzI*

antibody. The blot shown in Figure 7, suggests that each mutant is expressed as in the case of wild type and exists as a covalently linked homodimer except for mutant R<sub>Z</sub>K76E. Another mutant R<sub>Z</sub>L72F exhibited a ladder with bands of higher or lower molecular mass implying the highly unstable nature of such mutation in R<sub>Z</sub>.

Similarly, the expression test for R<sub>Z</sub>1 mutants was conducted (Figure 7). The blot obtained suggests that the mutants express R<sub>Z</sub>1 and that it exists as a homodimer linked covalently as in the case of R<sub>Z</sub>. However, we were not able to obtain strong bands for the positive and negative controls possibly due to errors in sample preparation. In the case of R<sub>Z</sub>1<sub>P35H</sub>, R<sub>Z</sub>1<sub>P36Q</sub>, R<sub>Z</sub>1<sub>P31L</sub> and R<sub>Z</sub>1<sub>P44S</sub> we either observed low levels of protein expression or none at all. Also, for the mutant R<sub>Z</sub>1<sub>W46C</sub>, we obtained a ladder-like expression pattern, showing bands of varying molecular masses possibly due to the unstable nature of this mutation similar to that observed in R<sub>Z</sub>L72F.

### **Mutants of R<sub>Z</sub> and R<sub>Z</sub>1 form a complex**

To further test if the mutations have any effect on the R<sub>Z</sub>-R<sub>Z</sub>1 interaction, a pull-down assay of selected non-functional R<sub>Z</sub> and R<sub>Z</sub>1 mutants was performed. We deliberately selected four mutants of R<sub>Z</sub> including one amber mutation at position 145 and one R<sub>Z</sub>1 mutant having a missense change towards the C-terminal end. We hoped that missense changes towards the C-terminal of the proteins would hinder the interaction between R<sub>Z</sub> and R<sub>Z</sub>1 and fail to form a complex since previous studies suggest that the C-terminal ends are important for R<sub>Z</sub>-R<sub>Z</sub>1 interaction (Berry et al., 2013). In this assay, we used a R<sub>Z</sub>1 allele that was tagged in-frame with a poly-Histidine (poly-His tag) residue at the C-terminal end. Such an allele has been shown to be functional in previous studies (Berry et al., 2008). Using Dynabeads (Invitrogen, Carlsbad,

CA) that specifically bind to His-tagged proteins, a complex was isolated. The isolated complexes were then examined by running a SDS-PAGE gel under reducing conditions followed by Western blotting (Figure 8). Compared to the wild type, all three Rz mutants, R91P, Q151R, and G143R were able to form a complex with Rz1-His. Similarly, Rz1<sub>I54N</sub>-His was also able to form a complex with Rz. However, a much more severely reduced amount of Rz<sub>G143R</sub> was detected in this assay. This might suggest that Rz<sub>G143R</sub> is not as efficient as other candidate to interact with Rz1. Since *Rz<sub>Q145am</sub>* results in the truncation of the C-terminal end of the protein, we did not detect its presence as a complex in this assay, as expected.

## CHAPTER IV

### DISCUSSION

To overcome the embedded genetic architecture complexity of the spanins genes, we separated the *Rz/RzI* genes in the  $\lambda$  chromosome. From previous studies we know that the spanin subunits interact with each other and undergo certain unknown conformational changes, which aid in spanin function (Berry et al., 2010). By introducing mutations in either gene, we hoped to isolate suppressors which would result in functional spanins. Previous studies have shown that isolating suppressors of introduced mutations can give substantial information about the interacting surfaces (Mortin, 1990). Hence the similar approach was used to understand the residues important for the spanins either for interaction or functionality.

However lack of prior information about which residues play an important role in spanin functionality, i.e. which mutations abolish spanin function, we decided to use the approach of creating a mutant library of either gene mutagenized to saturation level. A feasible method of doing so was the approach of random mutagenesis using error-prone PCR rather than working with one mutation one at a time. Interestingly, two of initially screened non-functional mutants *Rz<sub>R83H</sub>* and *RzI<sub>K96I</sub>*, were determined to be functional mutants as they complemented for *Rz<sub>am</sub>* in the lysogen and caused lysis of the culture. We can assume that these regions of *Rz* probably do not participate in the steps of spanin functioning, which is why they fail to block lysis. Other possible reasons could be attributed to the fact that arginine and histidine are both basic and polar in the case of *Rz<sub>R83H</sub>* and hence interchangeable, while for *Rz<sub>K96I</sub>* the mutation does not occur

near any sites that participate in the predicted secondary structure formation and presumably does not affect Rz conformation in a detrimental manner.

We characterized these mutants biochemically in order to confirm their expression level and if they were dominant over the wild-type spanins as low expression levels could explain why the functionality is abolished. Interestingly, all the mutants were revealed to be recessive and did not affect the existing wild-type spanins of the plasmid into which they were transformed.

Most of the spanin mutants tested did not have defects in level of expression and also existed as covalently linked homodimers just as in the case of the wild-type spanins. However, we did obtain cases of poor expressions namely Rz<sub>L72F</sub>, Rz<sub>K76E</sub> and Rz<sub>K96I</sub>. The mutation Rz<sub>K76E</sub> lies in the antigenic region of Rz and results in the conversion from basic lysine to acidic glutamic acid. This could explain the lack of a band in Rz<sub>K76E</sub> as the mutation possibly results in an altered structure that hinders the binding of the epitope. However we cannot rule out the possibility of this mutation causing instability of the Rz protein. Although Rz<sub>L72F</sub> also lies near the antigenic region of Rz, it does not affect the antibody binding as severely as in the case of Rz<sub>K76E</sub>. However from the detected ladder-like pattern of Rz<sub>L72F</sub>, we can assume that the mutation results in a highly unstable Rz protein. Also, the mutations Rz<sub>L72F</sub> and Rz<sub>K76E</sub> both lie in the predicted  $\alpha$ -helical domain of the Rz protein and hence mutations in this region could affect the spanin function. The mutation K96I results in weaker expression of Rz compared to the other mutants. This mutation however is associated with wild-type behavior and has no effect on the functionality of the spanin since it causes lysis of the culture as shown in Table 3a. Hence we

know that the protein is expressed although its proximity to the antigenic region could possibly affect its recognition by the antibody resulting in a faint band.

In the case of *Rz1* mutant expression analysis, no bands were detected in the case of *Rz1*<sub>P35H</sub> and *Rz1*<sub>P36Q</sub>. Both these mutations lie in the antigenic region of *Rz1* and possibly alter the protein conformation in a way that causes them to not be detected by the *Rz1* specific antibody although the possibility that these mutants fail to express *Rz1* also exists. Interestingly, a faint band was detected for the mutant *Rz1*<sub>P31L</sub> even though it exists in the same region. This could possibly be due the fact that leucine is a non-polar residue like proline unlike histidine and glutamine and hence does not affect the conformation as severely. A faint band was also detected in the case of *Rz1*<sub>P44S</sub> possibly again due to the change in polarity of the residue at that site resulting in weak expression. Another important mutant to note is *Rz1*<sub>W46C</sub> as it is detected as a ladder like oligomeric pattern, which could mean that this mutation results in a highly unstable protein. We also cannot rule out improper sample preparation due to human error due to the fact that we were unable to detect bands in the case of the controls when probed against *Rz1*.

Since the other mutants were determined to be non-functional as well as recessive, we expected the spanin interaction to be blocked in these mutants which would explain their non-functionality. We were however, only able to detect low amounts of interaction in one mutant, *Rz*<sub>G143R</sub>, and wild-type interaction levels in others. Hence we can say that there are multiple steps in the spanin function pathway, apart from the spanin interaction step.

The genetic and biochemical characterization of any gene responsible for a particular function can give us insight into the specific mechanism by which the gene functions. While we know that the spanins are required for the disruption of the outer membrane, the exact mechanism of this step is still unknown. Models based on genetic, biochemical, and biophysical properties of the spanins point towards membrane fusion of the OM and the IM. However, critical details such as the residues that participate in this step as well as structural rearrangements that might take place are still largely unknown.

Spanins are not the only fusion proteins. Eukaryotic membrane vesicles also undergo fusion in order to transmit signals (Vardjan et al., 2009). The Influenza virus is one of the membrane bound viruses that utilizes membrane fusion to enter the host cell (Kempf et al., 1987). In both cases, the exact mechanisms are still unknown. Nevertheless, the spanins are the only proteins shown to cause fusion between distinct membranes in prokaryotic systems (*Rajaure M. et al., unpublished*) and thus may be a good system for the study of this important process. Although our study did not give us the desired results, we hope that the direction of this study will help in answering key questions.

## REFERENCES

- Barik, S. (2002). Megaprimer PCR. *Methods in molecular biology* 192, 189-196.
- Bernhardt, T.G., Roof, W.D., and Young, R. (2002). The Escherichia coli FKBP-type PPlase SlyD is required for the stabilization of the E lysis protein of bacteriophage phi X174. *Molecular microbiology* 45, 99-108.
- Berry, J., Rajaure, M., Pang, T., and Young, R. (2012). The spanin complex is essential for lambda lysis. *Journal of bacteriology* 194, 5667-5674.
- Berry, J., Savva, C., Holzenburg, A., and Young, R. (2010). The lambda spanin components Rz and Rz1 undergo tertiary and quaternary rearrangements upon complex formation. *Protein science : a publication of the Protein Society* 19, 1967-1977.
- Berry, J., Summer, E.J., Struck, D.K., and Young, R. (2008). The final step in the phage infection cycle: the Rz and Rz1 lysis proteins link the inner and outer membranes. *Molecular microbiology* 70, 341-351.
- Berry, J.D., Rajaure, M., and Young, R. (2013). Spanin function requires subunit homodimerization through intermolecular disulfide bonds. *Molecular microbiology* 88, 35-47.
- Cirino, P.C., Mayer, K.M., and Umeno, D. (2003). Generating mutant libraries using error-prone PCR. *Methods in molecular biology* 231, 3-9.
- Kedzierska, S., Wawrzynow, A., and Taylor, A. (1996). The Rz1 gene product of bacteriophage lambda is a lipoprotein localized in the outer membrane of Escherichia coli. *Gene* 168, 1-8.
- Kempf, C., Michel, M.R., Kohler, U., and Koblet, H. (1987). Can viral envelope proteins act as or induce proton channels? *Bioscience reports* 7, 761-769.
- Kolisnychenko, V., Plunkett, G., 3rd, Herring, C.D., Feher, T., Posfai, J., Blattner, F.R., and Posfai, G. (2002). Engineering a reduced Escherichia coli genome. *Genome research* 12, 640-647.
- Mortin, M.A. (1990). Use of second-site suppressor mutations in Drosophila to identify components of the transcriptional machinery. *Proceedings of the National Academy of Sciences of the United States of America* 87, 4864-4868.



Park, T., Struck, D.K., Deaton, J.F., and Young, R. (2006). Topological dynamics of holins in programmed bacterial lysis. *Proceedings of the National Academy of Sciences of the United States of America* 103, 19713-19718.

Peters, J.E., Thate, T.E., and Craig, N.L. (2003). Definition of the *Escherichia coli* MC4100 genome by use of a DNA array. *Journal of bacteriology* 185, 2017-2021.

Schagger, H., and von Jagow, G. (1987). Tricine-sodium dodecyl sulfate-polyacrylamide gel electrophoresis for the separation of proteins in the range from 1 to 100 kDa. *Analytical biochemistry* 166, 368-379.

Smith, D.L., Chang, C.Y., and Young, R. (1998). The lambda holin accumulates beyond the lethal triggering concentration under hyperexpression conditions. *Gene expression* 7, 39-52.

Summer, E.J., Berry, J., Tran, T.A., Niu, L., Struck, D.K., and Young, R. (2007). Rz/Rz1 lysis gene equivalents in phages of Gram-negative hosts. *Journal of molecular biology* 373, 1098-1112.

Vardjan, N., Jorgacevski, J., Stenovec, M., Kreft, M., and Zorec, R. (2009). Compound exocytosis in pituitary cells. *Annals of the New York Academy of Sciences* 1152, 63-75.

Zhang, N., and Young, R. (1999). Complementation and characterization of the nested Rz and Rz1 reading frames in the genome of bacteriophage lambda. *Molecular & general genetics* : MGG 262, 659-667.

## APPENDIX

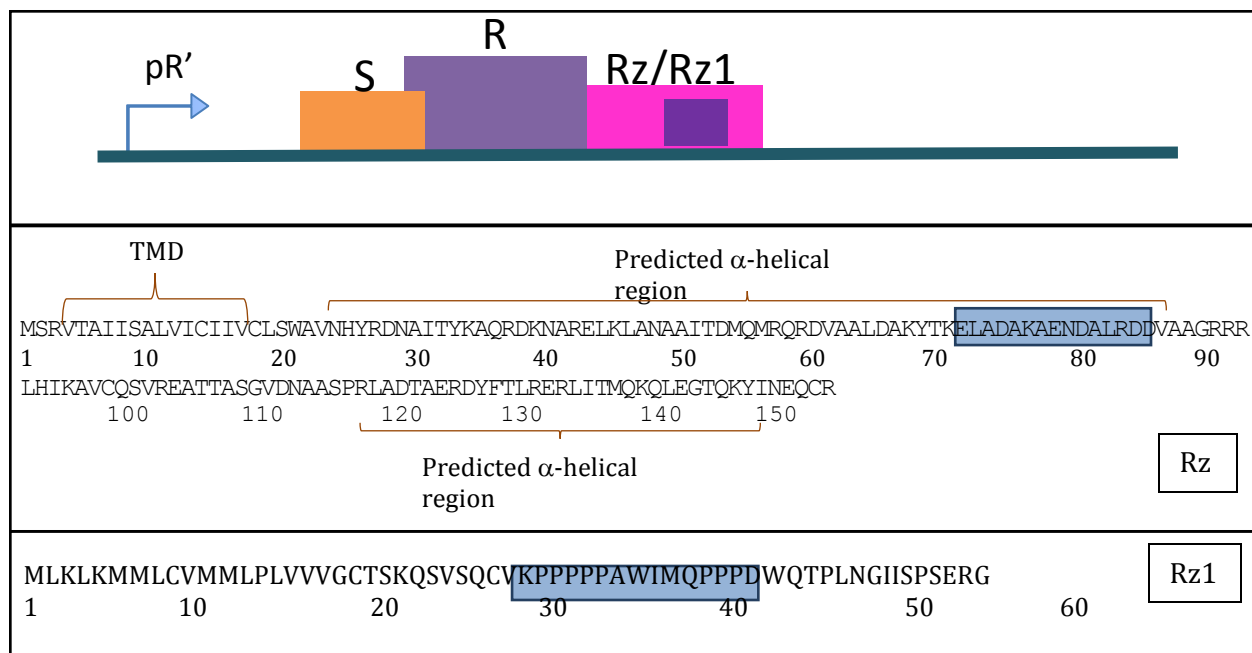


**Figure 1. The Spanin genes of  $\lambda$ .** The  $\lambda$  lysis cassette shown downstream of the  $\lambda$  late promoter  $pR'$  (top) and the amino acid sequences of  $Rz$  (center) and  $Rz1$  (bottom). The transmembrane regions and predicted secondary structures of  $Rz$  are as marked and the blue boxed text represents the antigenic regions of the respective proteins.

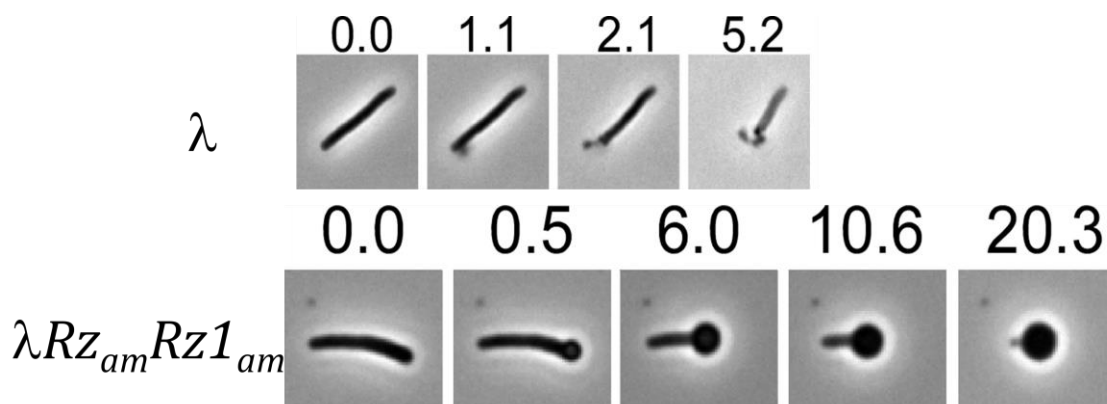


**Figure 2. Spanin mediated  $\lambda$  lysis.** Time lapse images (in seconds) showing the effects of spanins on the cells. The top panel displays the rapid lysis in the case of wild-type  $\lambda$ . The spherical cell phenotype is observed in defective spanins (bottom) (Berry et al., 2012)

**Table 1. Genotypes of the strains used.**

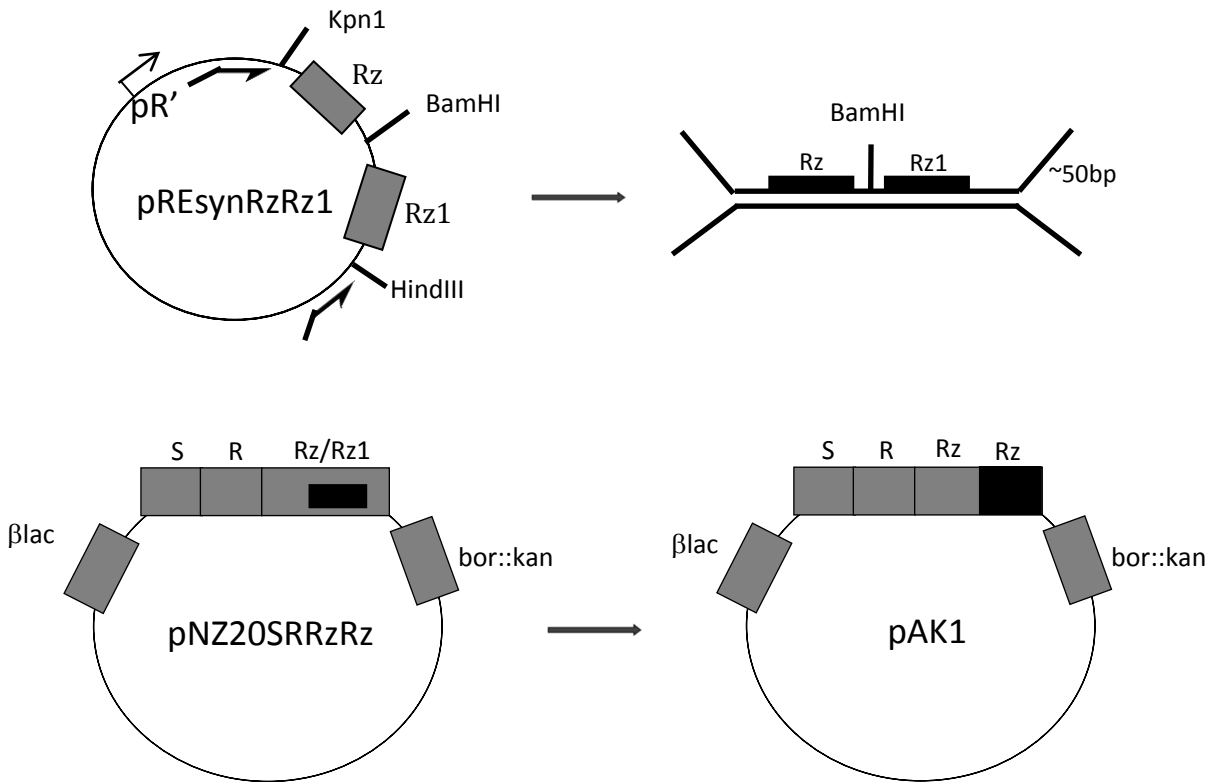
	Genotype and relevant features	Sources, References
<b>Bacteriophages</b>		
$\lambda$ 900	$\lambda\Delta(stf\ tfa)::cat\ cI_{857}\ bor::kan$ ; carries Cam <sup>R</sup> and Kan <sup>R</sup> ; $R_z^+R_zI^+$	(Zhang and Young, 1999)
<b><i>E. coli</i> K-12 strains</b>		
MDS-12	Reduced (8.1% in size and 9.3% in gene count) genome strain using <i>E.coli</i> K-12 strain MG1655 (F- $\lambda$ - <i>ilvG</i> - <i>rfb</i> -50 <i>rph</i> - 1).	(Kolisnychenko et al., 2002)
MC4100	<i>[araD139]B/r</i> , <i>Del(argF-lac)169</i> , <i>e14</i> -, <i>flhD5301</i> , $\Delta(fruK\text{-}yeiR)725(fruA25)$ , <i>relA1</i> , <i>rpsL150(strR)</i> , <i>rbsR22</i> , <i>Del(fimB-fimE)632(::IS1)</i> , <i>deoC1</i>	(Peters et al., 2003)
MC4100 ( $\lambda$ 900)	Lysogen carrying $\lambda$ 900prophage	This study

Table 1 continued

Plasmids		
pRE	Derivative of pJF118EH with $\text{lacI}^Q$ and Ptac promoter replaced with pR' promoter region of $\lambda$ ; transcriptionally activated by $\lambda Q$	(Park et al., 2006)
pNZ20 $\lambda$ <i>SRRzRzI</i>	Plasmid cloned to contain the parental $\lambda$ lysis cassette; carries $\text{Amp}^R$ and $\text{Kan}^R$	This study
pAK1	Plasmid constructed using pNZ20 $\lambda$ <i>SRzRz</i> having synthetic and separate <i>Rz-RzI</i> alleles; carries $\text{Amp}^R$ and $\text{Kan}^R$	This study

**Table 2: Primers used for site-directed mutagenesis.**

Mutation	Direction	Sequence
RzL93S	Forward	5' gcggcgccgatcacatattaagg 3'
	Reverse	5' ccttaatatgtgatcggcgccgc 3'
RzD65G	Forward	5' tgctgcgctctaggcaaaataca 3'
	Reverse	5' tgtattttgcctagagcgcagca 3'
RzQ151R	Forward	5' attaatgagcgggtgcagatag 3'
	Reverse	5' ctatctgcaccgtcattaat 3'
RzL72F	Forward	5' acgaaggagttcgctgacgcc 3'
	Reverse	5' ggcgtcagcgaactccttctg 3'
RzG143R	Forward	5' acaactggaagaaccagaagt 3'
	Reverse	5' acttctgggttcttccagttgt 3'
RzY147H	Forward	5' aaccagaagcatattaatgagc 3'
	Reverse	5' gctcattaatatgcttctgggtt 3'
RzI154N	Forward	5' aaatggaatcaaatcgccatcgg 3'
	Reverse	5' ccgatggcgatttgattccattt 3'



**Figure 3.a. Construction of plasmid pAK1.** The pR' plasmid cloned with synthetic *Rz* and *Rz1* alleles (top left); Amplification of the synthetic *Rz-Rz1* region to obtain mega-primer (top right) with flanking regions (~50bp) homologous in frame to the upstream and downstream sequence of *Rz* and *Rz1* respectively (bottom left); Newly constructed pAK1 plasmid (bottom right).

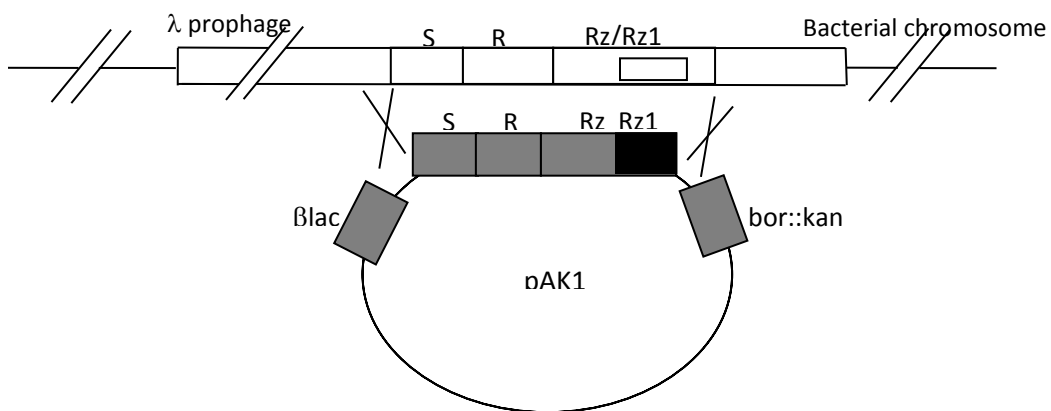


**Figure 3.b. Phage construction using pAK1 plasmid.** Homologous recombination between plasmid pAK1 (bottom) and a λ lysogen containing parental λ lysis cassette (top).

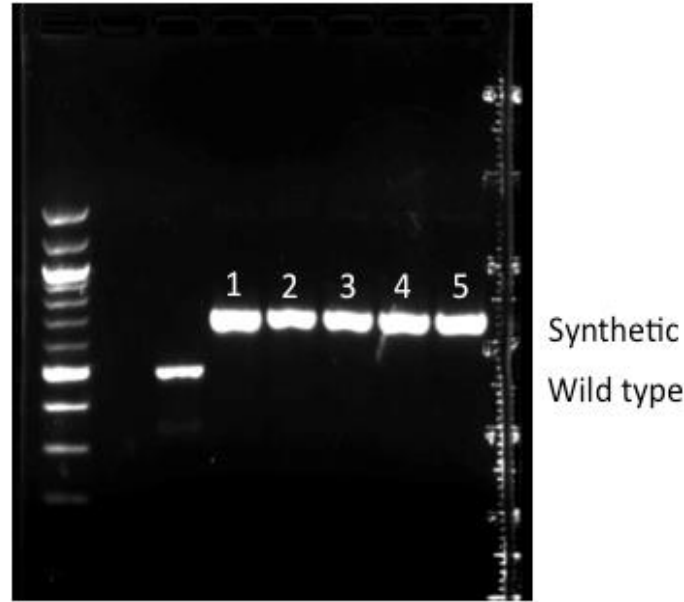


**Figure 3.c. Comparison of  $\lambda$  parental and synthetic spanins.** The PCR product of 462bp long DNA fragment of embedded spanin genes (lower band). The PCR product of 662 bp long DNA fragment of synthetic Rz and Rz1 in tandem separated by 19 bp nucleotide. The synthetic alleles numbered 1-5 are  $\lambda_{\text{synRzQ151R}}$  Rz1,  $\lambda_{\text{synRzL93S}}$  Rz1,  $\lambda_{\text{synRzD65G}}$  Rz1,  $\lambda_{\text{synRzL72F}}$  Rz1 and Synthetic  $\lambda_{\text{RzRz1}}$  in order. First lane represents 100bp DNA ladder.

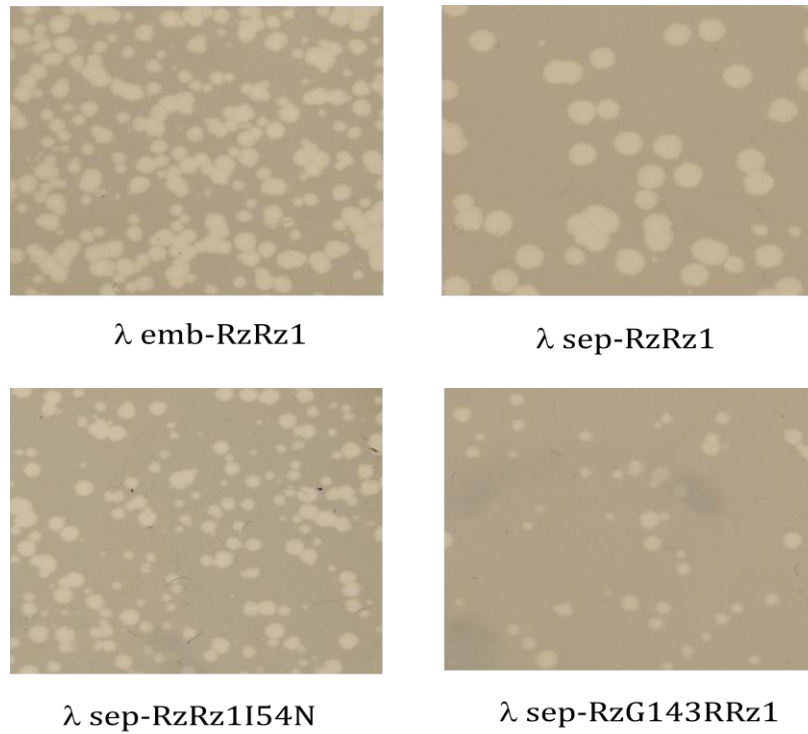


**Figure 4. Comparison of plaque sizes in  $\lambda$  chromosomes with different spanin alleles.** The  $\lambda$ cI857 chromosomes containing the wild-type embedded spanin and the synthetic separated spanin alleles with (top) give almost similar large size plaques. The reduced punctiform plaques due to I54N mutation in Rz1 and G143R mutation in Rz (bottom).



**Table 3. Genetic characterization of non-functional mutants from the *Rz* and *Rz1* pools.**

3.a) *Rz* mutants

Mutant ID	Position	Lysis <sup>a</sup>	Dominant/ Recessive
1	R91P	-	Recessive
10	R83H	+	Recessive
16	K96I	+	Recessive
28	V61A	- <sup>b</sup>	Recessive
62	K76E	-	Recessive
69	K146N	-	Recessive
103	L64R	-	Recessive
104	A73V	-	Recessive
107	V86G	-	Recessive
217	L64H	-	Recessive
218	D65G	-	Recessive
230	Q151R	-	Recessive
259	L93S	-	Recessive
266	L72F	-	Recessive
269	Y147H	-	Recessive
284	G143R	-	Recessive

3.b) *Rz1* mutants

Mutant ID	Mutation	Lysis	Dominant/ Recessive
3	P35H	-	Recessive
8	P36Q	-	Recessive
9	L50R	-	Recessive
10	W46R	-	Recessive
16	C9S	-	Recessive
21	P33L	-	Recessive
22	L50P	-	Recessive
31	L50P	-	Recessive
39	W46C	-	Recessive
46	P44S	-	Recessive

a - Here '+' denotes lysis of the culture and '-' denotes a non-lyser.

b - The mutant Q145st was determined to be a slow lyser.

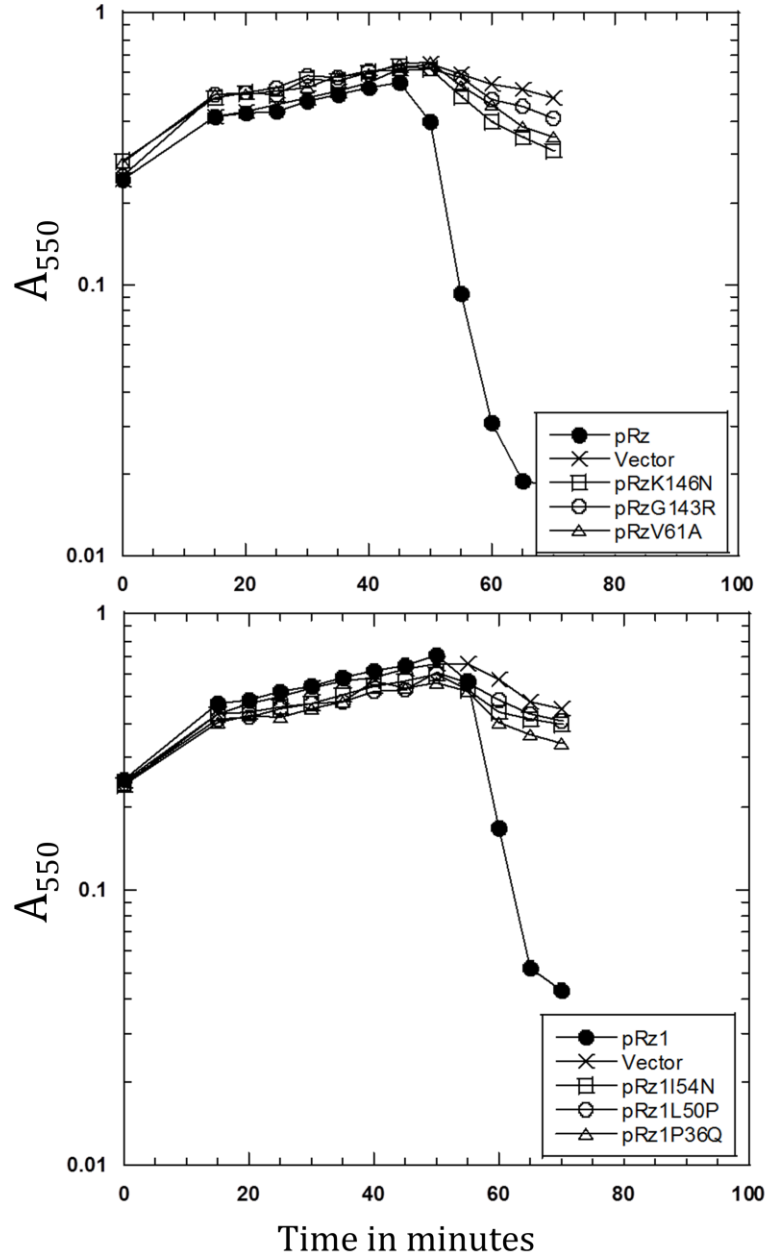


**Figure 5. Representative mutants that do not complement the spanin defective lysis.** The *Rz* mutant lysis profiles are shown in (a) and the *RzI* mutants are shown in (b). The induced expression of *Rz* and *RzI* in the host background of *MC4100*  $\lambda$  *Rz<sub>am</sub>* and *MC4100*  $\lambda$  *RzI<sub>am</sub>*, respectively, caused lysis (black circles) whereas absence of complementary spanin subunit blocked lysis (vector, x). The non-functional mutants that were unable to complement the corresponding spanin defects are labeled in the inset.



**Figure 6. Mutagenization of spanins to saturation level.** The non-sense mutations are denoted by ‘\*’ for *Rz* (top) and *Rz1* (bottom).

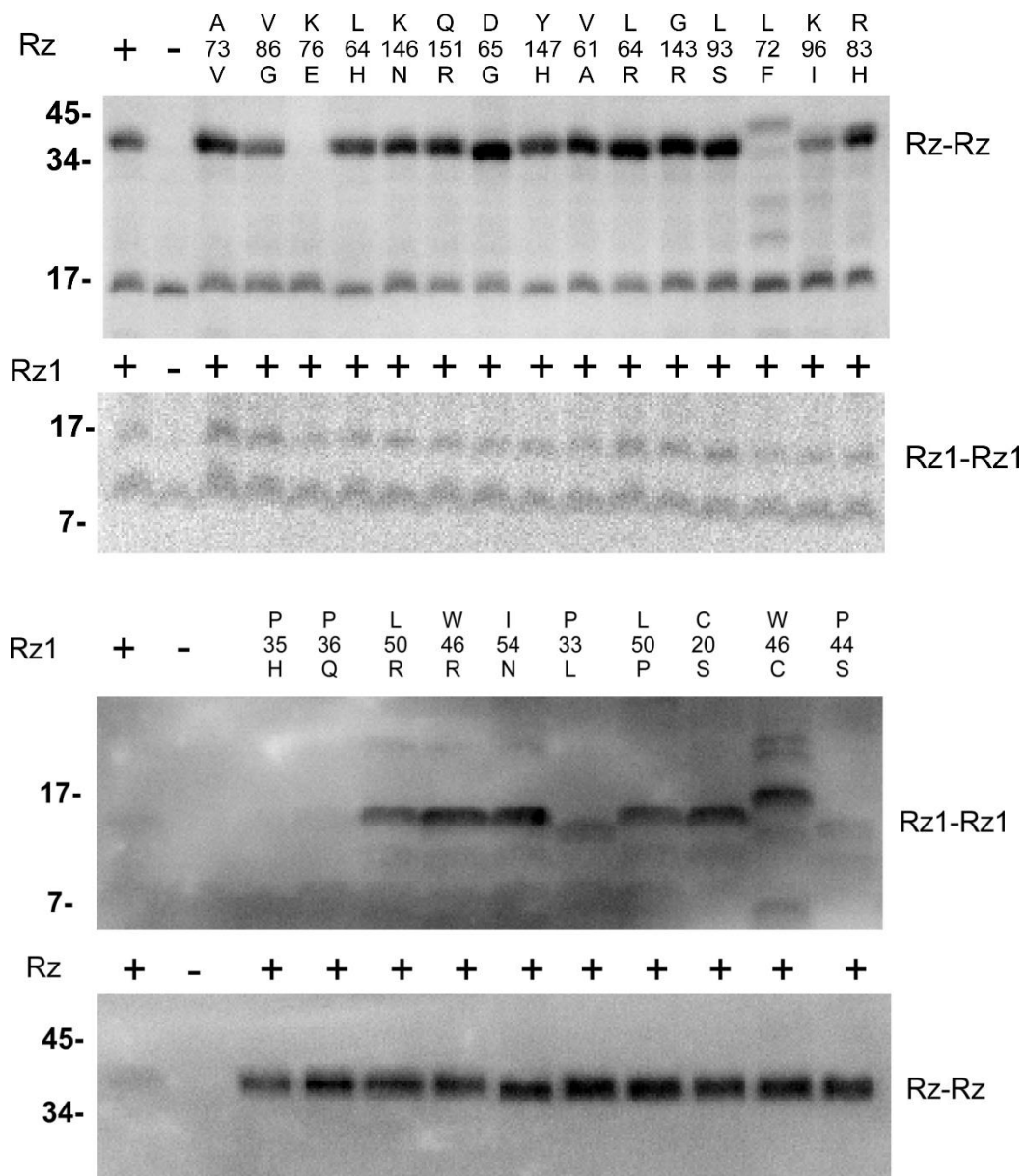


**Figure 7. Most mutants of Rz and Rz1 are not affected for its accumulation *in-vivo*.** TCA precipitates of induced Rz (top panel) and Rz1 (bottom panel) in the presence of their respective interacting partner (lower blot in each panel) were assessed by SDS-PAGE under non-reducing conditions followed by Western blotting. The amino acid changes are indicated at the top, “+” and “-” sign indicates the positive and negative control, respectively. Molecular mass marker is indicated in the left.

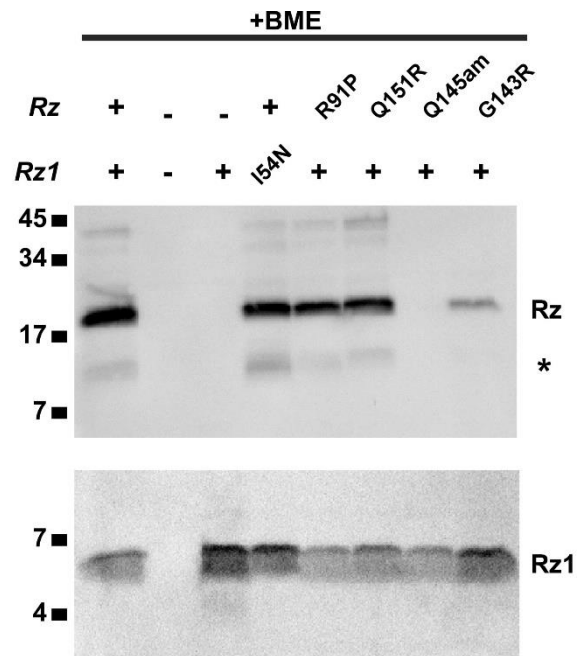


**Figure 8. Mutants did not affect the Rz-Rz1 interaction.** Isolated complex of the selected spanin mutants, using Rz1-His tagged proteins, was assessed by SDS-PAGE under reducing conditions followed by Western blotting. The Rz or Rz1-His allele are indicated at the top. The probed Rz and Rz1 signals are indicated in the right. First three lanes represent the positive, negative, and Rz1-His controls.